JOURNAL OF MATERIALS SCIENCE 28 (1993) 1849–1855

# Mode I interlaminar fracture toughness of commingled carbon fibre/PEEK composites

HOGYU YOON, KIYOHISA TAKAHASHI
*Department of Materials Science and Engineering, Nagoya Institute of Technology, Gokiso-cho, Showa-ku, Nagoya 466, Japan*

Carbon fibre/poly (ether-ether-ketone) (PEEK) composites were fabricated from plain weave cloth using the commingled yarn of carbon fibres with PEEK filaments. The undirectional specimen was made from the warp of commingled yarn and the weft of PEEK yarn, while the two-dimensional specimen was made from commingled yarns both of the warp and the weft. During the hot-pressing process, PEEK filaments melt to form the matrix of the composite. The interlaminar fracture toughness of the commingled composite was measured and compared with that of the prepreg composite. The critical strain energy release rates, $G'_{1c}$s, obtained for the commingled composites were higher than the prepreg composite. In particular, the two-dimensional composite exhibited higher $G_{1c}$ than the unidirectional commingled composite. Factors increasing the fracture toughness of commingled composites have also been investigated by SEM observation of the fractured surface.

## 1. Introduction

In the application of advanced polymeric composites, poly(ether-ether-ketone) (PEEK) offers a number of significant advantages over the conventional thermosetting polymers such as epoxy resin. Carbon fibre (CF)/PEEK composites have attracted much attention in many applications [1, 2], because of their outstanding fracture toughness, heat resistance, moisture resistance and storage stability. Because the melting temperature of PEEK resin, 335 °C, is very high, CF/PEEK composites have the advantage of being available for high-temperature service. However, the high melting temperature and the high melt viscosity of PEEK resin give rise to difficulty in the fabrication of the composite. In order to help the melted PEEK to impregnate into the carbon fibres and to make the homogeneous composite, mainly the prepreg has been used. The fabrication method using commingled yarn instead of the prepreg has also been investigated [3, 4]. The commingled yarn has an advantage over the prepreg in that near-net-shape preforms of complicated shapes of composite can be fabricated by weaving or braiding technique; for example, three-dimensional structural composites [5].

Much work has been carried out to characterize the fracture toughness of CF/PEEK and CF/epoxy composites [6–9], as shown in Table I. The critical strain energy release rate of the CF/PEEK composites is around 1800 $J m^{-2}$, and it is six to ten times larger than that of CF/epoxy composite. This is mainly due to the matrix property. That is, the PEEK resin is tough and ductile, while the epoxy resin is brittle. These experimental data were obtained for specimens made of prepreg materials. In the present work, unidirectional and two-dimensional CF/PEEK composites were manufactured with commingled yarns. The interlaminar fracture toughness was measured and compared with that of the CF/PEEK prepreg composite. Scanning electron microscopic (SEM) observation was employed in order to examine the impregnation of PEEK resin into the cabon fibres and the interfacial adhesion between them. The effect of fibre alignments on the fracture toughness of the composites was also investigated.

## 2. Experimental procedure

### 2.1. Commingled yarn

The commingled yarn (1800 denier; Schappe Co., France) was composed of carbon and PEEK fibres. The carbon and PEEK filaments were cut by the stretch-breaking method in lengths of about 12 cm. These staples were spun to form the commingled yarn. Fig. 1a shows a scanning electron micrograph of the

TABLE I Fracture toughness of CF/PEEK and CF/epoxy prepreg composite reported in the literature [6–9]

| Composite | $G_{1c}$ ($J m^{-2}$) |
|---|---|
| CF/PEEK prepreg | 1990 [6]<br>1750 ± 130 [9]<br>1650 [7] |
| CF/epoxy prepreg | 190 ± 30 [9]<br>257 [8] |

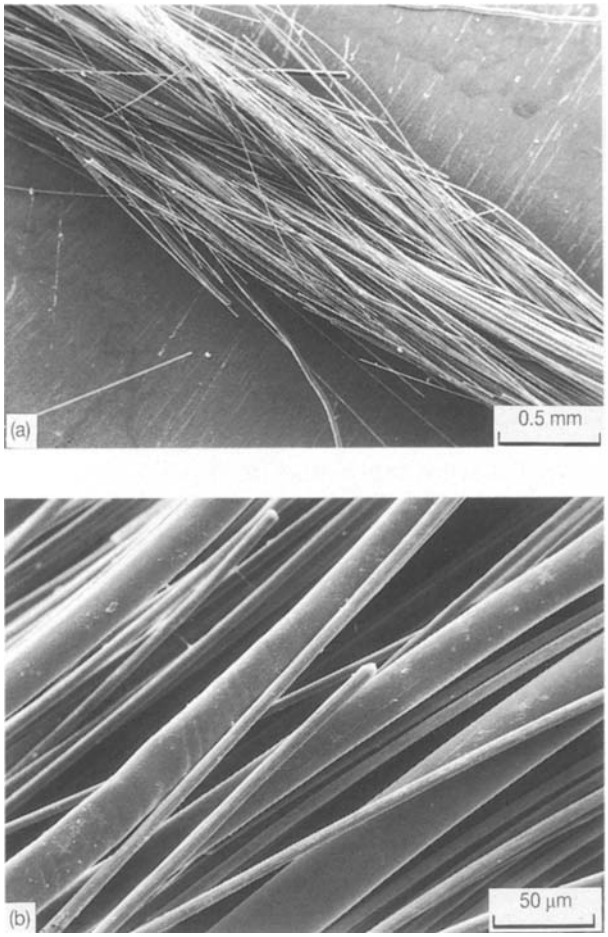


*Figure 1* (a) Commingled yarn of carbon fibre with PEEK fibre. (b) Magnification of (a). The thicker fibres are PEEK and the thinner fibres are carbon.

commingled yarn (two-ply yarn). A magnification of Fig. 1a is shown in Fig. 1b, in which the thicker fibres are PEEK and the thinner ones are carbon. Tips of carbon fibres protrude from the yarn as fluff. During the hot-pressing process, the PEEK fibres melt to form the matrix of the composite. Then, bonding between the matrix and the carbon fibres and hence adhesion between the neighbouring laminae, are expected to increase due to the presence of this fluff. As a result, an improvement in the fracture toughness is expected.

## 2.2. Laminae

The CF/PEEK laminae used for the experiment were as follows.

(a) Prepreg: the unidirectional CF/PEEK prepreg; APC-2 (Imperial Chemical Industries, ICI). The volume fraction of carbon fibre was 62 %.

(b) Unidirectional (UD) commingled: the plain-weave cloth was composed of the warp of CF/PEEK commingled yarn (1800 den) and the weft of PEEK yarn (70 den, Teijin Co.) as shown in Fig. 2. The volume fraction of carbon fibre in the commingled yarn was 63 %, while that in the plain-weave cloth was 60 %.

(c) Two-dimensional (2D) commingled: the plain-weave cloth was composed of commingled yarns for both warp and weft. The volume fraction of carbon fibre was 62 %–63 %.

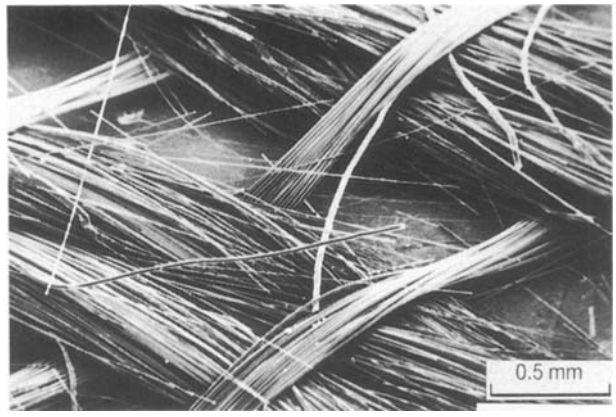


*Figure 2* Plain-weave cloth of commingled yarn and PEEK yarn. Warp is commingled yarn (1800 den) of carbon fibre with PEEK fibre, and weft is PEEK yarn (70 den).

## 2.3. Composite

The CF/PEEK composite laminates were packed into a vacuum bag of polyimide (Upirex, Ube Kosan Co.) and inserted between the hot steel plates preheated at 200 °C on which the mould release agent (Free Coat 44, Hiraizumi Yoko Co.) was coated. The temperature was raised to 400 °C at a rate of 2.5 °C $min^{-1}$ under constant pressure. To prevent oxidation, nitrogen gas was introduced into the vaccum bag. The temperature was then lowered to about 100 °C by natural cooling (about 2 °C $min^{-1}$) to give the final specimen. The pressure applied to the prepreg composite was 6 kg $cm^{-2}$, while the UD commingled and the 2D commingled composites were pressed under 20 and 50 kg $cm^{-2}$, respectively, in order to suppress the void formation.

Fig. 3 illustrates the procedure to make the unidirectional commingled composite. In the case of 2D commingled composite, CF/PEEK commingled yarns were used for both warp and weft.

## 2.4. Measurement

To measure the mode I interlaminar fracture toughness, double cantilever beam (DCB) specimens were used. The geometry of a DCB specimen is shown in Fig. 4. A very sharp starter crack was introduced by inserting a polyimide film ( $\simeq$ 20 μm thick) between the centre laminae of the composite. The size of the test specimen was 25.4 mm wide ($B$), 2 mm thick ($2h$) and 150 mm long. The load was applied to the specimen at a crosshead speed of 0.5 mm $min^{-1}$, through the steel hinge and aluminium block glued to the specimen. The crack propagated along the carbon fibre or in the warp direction.

## 2.5. Fracture toughness

Fracture toughness of the specimen was estimated by the critical strain energy release rate. When a crack

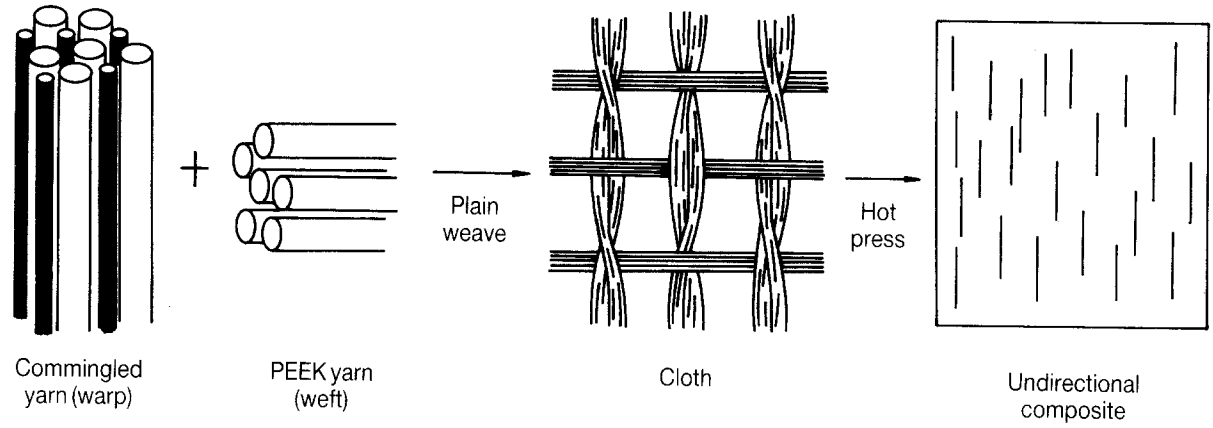


*Figure 3* A schematic illustration of fabrication procedure of unidirectional commingled composite. During the hot pressing, the PEEK yarn melts to form the matrix of the composite. In the case of 2D commingled composite, the weft of PEEK yarn is replaced by the CF/PEEK commingled yarn.

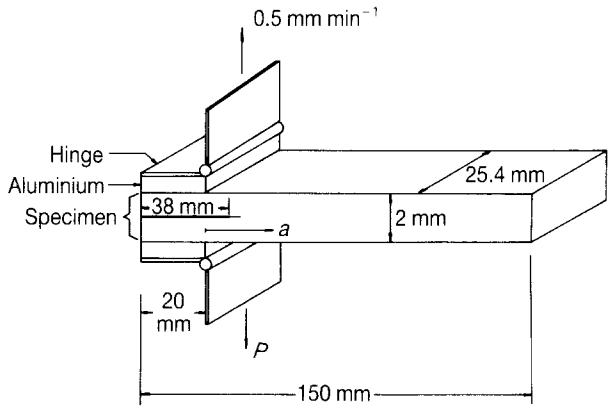


*Figure 4* Geometry of the double cantilever beam specimen used for the measurement of fracture toughness.

propagates in an elastic body under external load, a constant energy is released to form the new surface. This energy per unit area is called the strain energy release rate, $G_I$

$$G_I = \frac{P^2 \partial C}{2B \partial \bar{a}} \quad (1)$$

where $P$ is the applied load, $B$ the specimen width, $C$ the compliance, and $\bar{a}$ the crack length. From the measured $P$-$\Delta$ curves ($\Delta$ is the load-point displacement), the compliance, $C$, can be obtained and plotted against the crack length, $\bar{a}$. Using the values of $\partial C/\partial \bar{a}$ obtained from the $C$–$\bar{a}$ curve, $G_I$ can be calculated using Equation 1. In this experiment, the relation between $C$ and $\bar{a}$ was approximated by [10]

$$C(\bar{a}) = R\bar{a}^n \quad (2)$$

where $R$ and $n$ are constants experimentally determined.

From Equations 1 and 2, the critical strain energy release rate is given by

$$G_{Ic} = \frac{nP_c^2 C(\bar{a})}{2B\bar{a}} \quad (3)$$

where $P_c$ is the load measured at the point where the crack initiates or reinitiates.

## 3. Results and discussion

### 3.1. Load–displacement curve

The typical load–displacement curves obtained are shown in Fig. 5. The prepreg composite showed stable crack growth (Fig. 5a), where the crack propagates slowly across the specimen. On the other hand, the 2D commingled composite exhibited typical unstable crack growth (Fig. 5b) due to the carbon fibres in the weft. The UD commingled composite showed the intermediate failure behaviour, which is rather close to the prepreg composite.

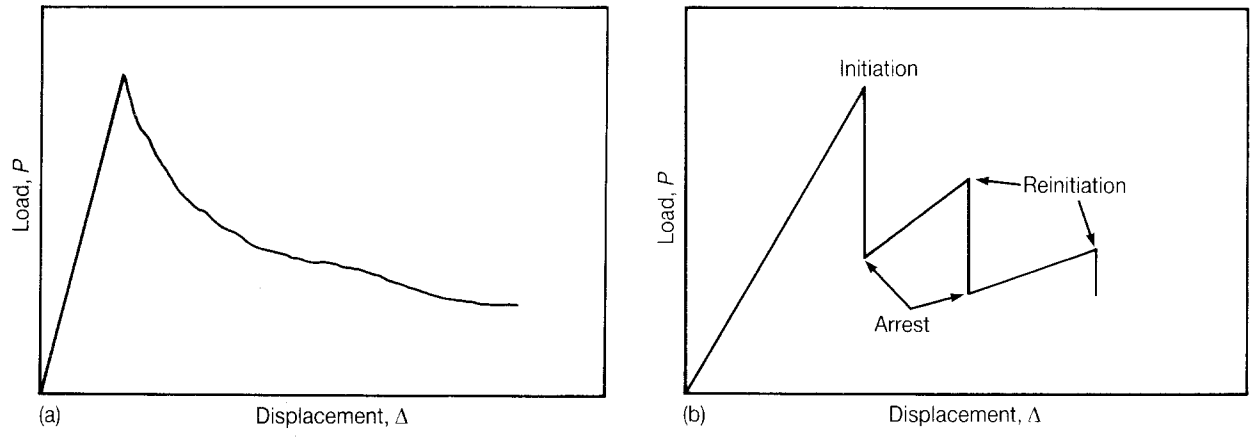


*Figure 5* Typical load–displacement curves for (a) stable crack growth and (b) unstable crack growth.

In the case of stable crack growth, the crosshead of the machine was stopped at the point where the crack extended about 10 mm. For the unstable crack growth, the machine was stopped at the points where the crack was arrested. Then the new crack tip was marked and the machine was unloaded to zero load. Again the load was applied and the crack propagated. This procedure was repeated.

The compliance, $C$, was calculated from the load–displacement curve and plotted against the crack length. Fig. 6 shows the typical $C$–$\bar{a}$ curves in double logarithmic plot. These relationships can be approximated by Equation 2. The values of $n$ were equal to 2.65 for the prepreg, 2.67 for the UD, and 2.64 for the 2D commingled composites, respectively. By substituting these values into Equation 3, the critical strain energy release rate is obtained. In the case of stable crack growth, the values of $G_{Ic}$ are calculated at the point of crack initiation and reinitiation, while in the case of unstable crack growth, the values of $G_{Ic}$ may be calculated at the point of crack initiation, reinitiation (propagation) and crack arrest.

## 3.2. Fracture toughness

Figs 7–9 show the critical strain energy release rate of the three types of composites as a function of the crack length. $G_{Ic}$ values were calculated at the point where the crack initiated or reinitiated. $G_{Ic}$ of the prepreg composite is approximately independent of the crack length (Fig. 7), while that of the UD (Fig. 8) or the 2D (Fig. 9) commingled composite depends on the crack length. In the range of small crack length, $G_{Ic}$ of the UD commingled composite is almost equal to that of the prepreg composite. However, for the crack length

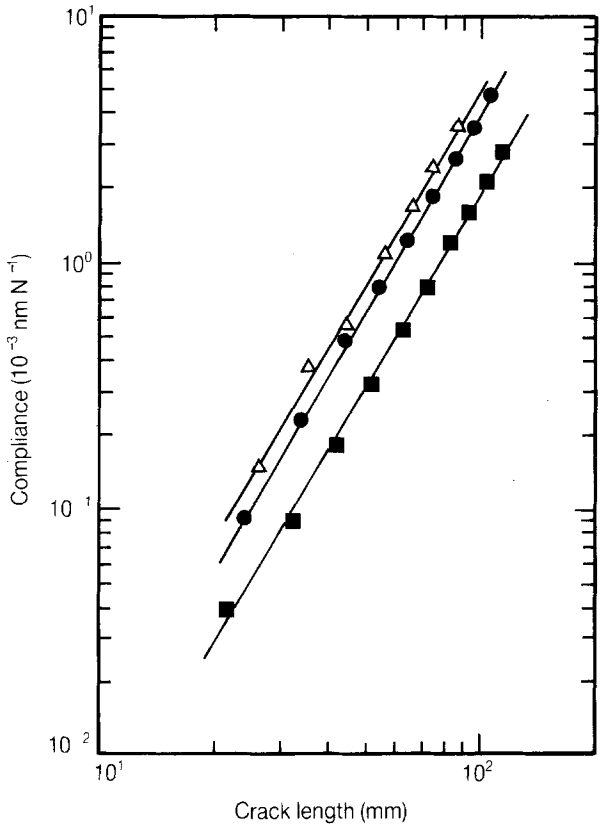


*Figure 6* Double logarithmic plot of the typical $C$–$\bar{a}$ relations, where $C$ is the compliance and $\bar{a}$ is the crack length. The slope $n = 2.65$ for the prepreg (■), 2.67 for the UD commingled (●) and 2.64 for the 2D commingled (△) composite, respectively.

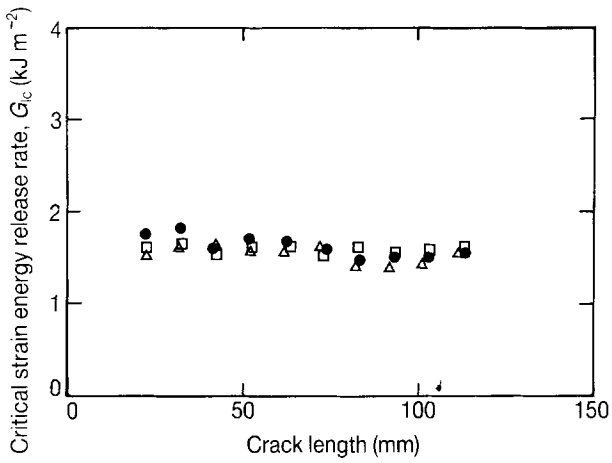


*Figure 7* Critical strain energy release rate, $G_{Ic}$, of the prepreg composite as a function of crack length. (●, □, △) Data obtained from three different test pieces.

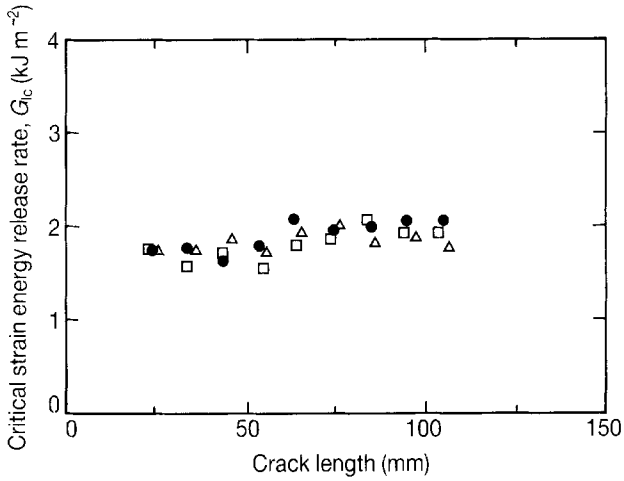


*Figure 8* Critical strain energy release rate, $G_{Ic}$, of the UD commingled composite as a function of crack length. (●, □, △) Data obtained from three different test pieces.

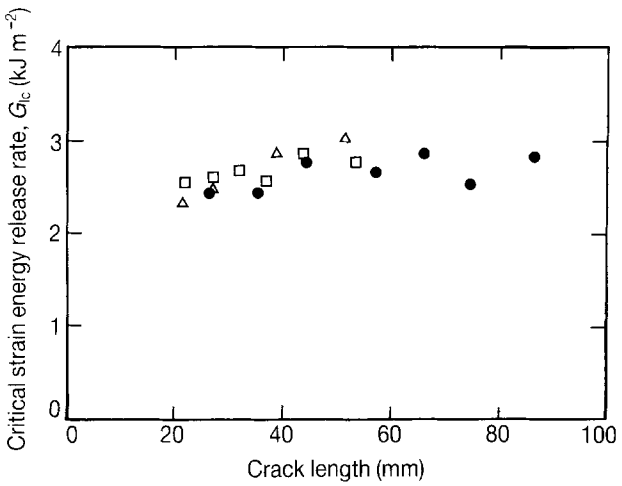


*Figure 9* Critical strain energy release rate, $G_{Ic}$, of the 2D commingled composite as a function of crack length. (●, □, △) Data obtained from three different test pieces.

more than 50 mm, higher $G_{Ic}$ values are obtained. This may be due to the increase of chances for fibre bridging or fibre breakage in the propagating region than the initiating region of the crack. The higher propagating $G_{Ic}$ compared with the initiating values is also found in the 2D commingled composite, which shows the highest fracture toughness of all of the three types of composite.

Because the fracture behaviour of the 2D commingled composite is very unstable, the fracture toughness can be calculated at the point of crack arrest as well as at the point of crack initiation or reinitiation as shown in Fig. 5b. In Fig. 10, $G^a_{Ic}$ calculated at the point of crack arrest was compared with $G^i_{Ic}$ at the crack initiation or $G^r_{Ic}$ at reinitiation. The $G^a_{Ic}$ value increases with crack length, and the average value is 1680 J m$^{-2}$. The results are summarized in Table II. The $G^a_{Ic}$ value of the unidirectional composites is equal to the reinitiation value and omitted here. It is interesting to note that the $G^a_{Ic}$ value of the 2D commingled composite is comparable to the $G^i_{Ic}$ or $G^r_{Ic}$ of the prepreg composite.

It was reported [11] that the glass/epoxy woven fabric composite has a fracture toughness of five to ten times higher than the unidirectional epoxy composite. In the present study, the $G_{Ic}$ values of the 2D commingled composite is only 1.5–2 times higher than the UD or the prepreg composite. This may be due to the high fracture resistance of neat PEEK resin.

## 3.3. SEM observations

First, the fracture surface of carbon fibre/epoxy composite is shown in Fig. 11 [12] for comparison with PEEK composites. Small fragmentations of epoxy resin between the carbon fibres indicate the typical brittle fracture. Because of the brittleness of the matrix, carbon fibre/epoxy composite is inferior to the carbon fibre/PEEK composite in the fracture toughness as shown in Table I.

The fracture surfaces of the prepreg and UD commingled composite are shown in Fig. 12a and b, respectively. The long tufts of resin can be observed.

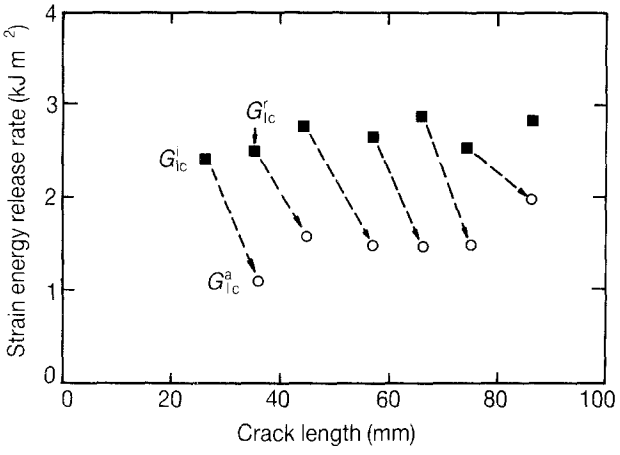


*Figure 10* Critical strain energy release rates, (○) $G^a_{Ic}$ at the point of crack arrest compared with ■ $G^i_{Ic}$ or $G^r_{Ic}$ at the point of crack initiation or reinitiation.

TABLE II The average values of the critical strain energy release rate obtained at the point of crack initiation, $G^i_{Ic}$, reinitiation, $G^r_{Ic}$, and arrest, $G^a_{Ic}$

| Composite | $G^i_{Ic}$ (initiation) (Jm$^{-2}$) | $G^r_{Ic}$ (reinitiation) (Jm$^{-2}$) | $G^a_{Ic}$ (arrest) (Jm$^{-2}$) |
|---|---|---|---|
| Prepreg | 1530 | 1560 | – |
| UD commingled | 1590 | 1980 | – |
| 2D commingled | 2320 | 2670 | 1680 |

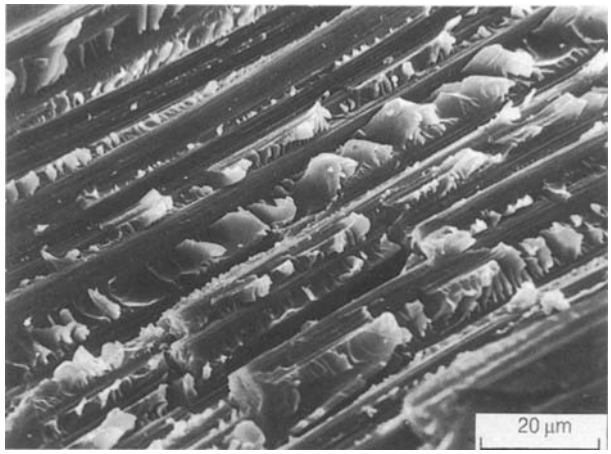


*Figure 11* SEM observation of the fracture surface of CF/epoxy composite made of Torayca prepreg P3060.

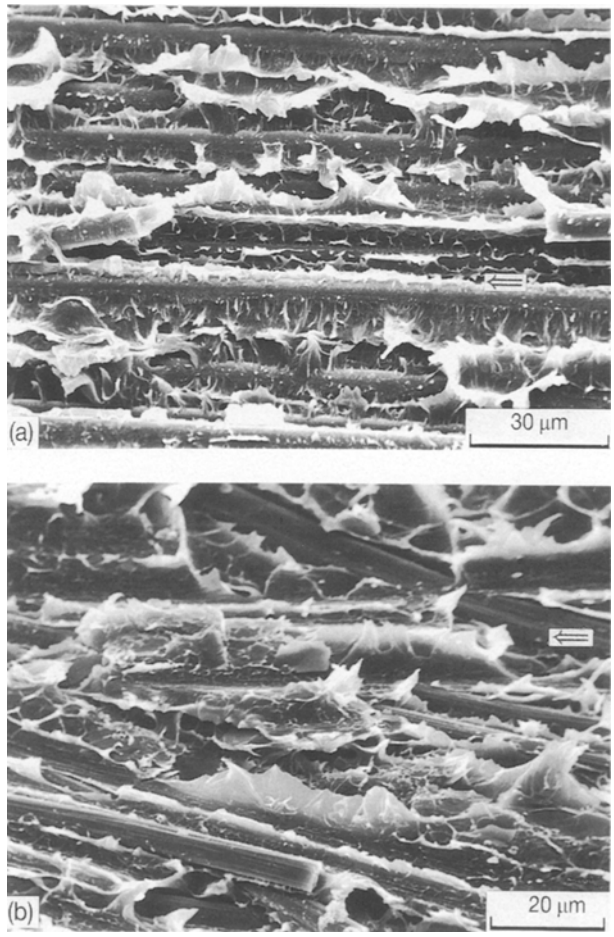


*Figure 12* SEM observation of the fracture surface of CF/PEEK composites. (a) The prepreg composite, and (b) the UD commingled composite. The arrow indicates the direction of crack propagation.

They indicate the ductile fracture of the PEEK resin and the good impregnation of resin into the carbon fibres. The appearance of the fracture surface of the prepreg composite, Fig. 12a, is uniform independently of the location and the fibres arrange parallel to each other. However, the fracture surface of the UD commingled composite, Figs. 12b and 13, is rough and irregular, and the fibres are misoriented. So, the chance for fibres to bridge between the crack faces is greater than the prepreg composite. This means that the crack propagation may be disturbed by the fibre bridging or by the ultimate fibre breakage. In Fig. 13b, the tips of broken carbon fibres are observed. Whether these carbon fibres were broken during the experiment or pulled out from the adjacent lamina is not clear. Anyway, these fibres certainly increase the fracture toughness of the commingled composites.

Fig. 14 shows the typical fracture surface of the 2D commingled composite. The crack propagated along the warp direction from right to left in Fig. 14a. The crack will be arrested in front of the weft carbon fibres (as indicated by A and B in Fig. 14a) before passing through the weft. The weft carbon fibres will be a barrier to the crack propagation (the delamination). Fig. 14b shows the ductile fracture of the PEEK resin just before the crack reaches the weft carbon fibres. There are weft carbon fibres and resin-rich parts on the left edge of Fig. 14b. It is supposed that the crack is arrested in front of the weft rib, and the matrix resin on the warp is elongated ductilely. In order to reinitiate the crack, more stress should be needed. The increased stress causes the rate of crack propagation to increase, which results in faster and unstable crack growth. Fig. 14c shows the fast crack propagation on the weft carbon fibres. The resin covering the weft carbon fibres shows a fine microductility which typically appears in the unstable failure surface.

Another feature of the fracture surface of the 2D commingled composite is that the delamination some-

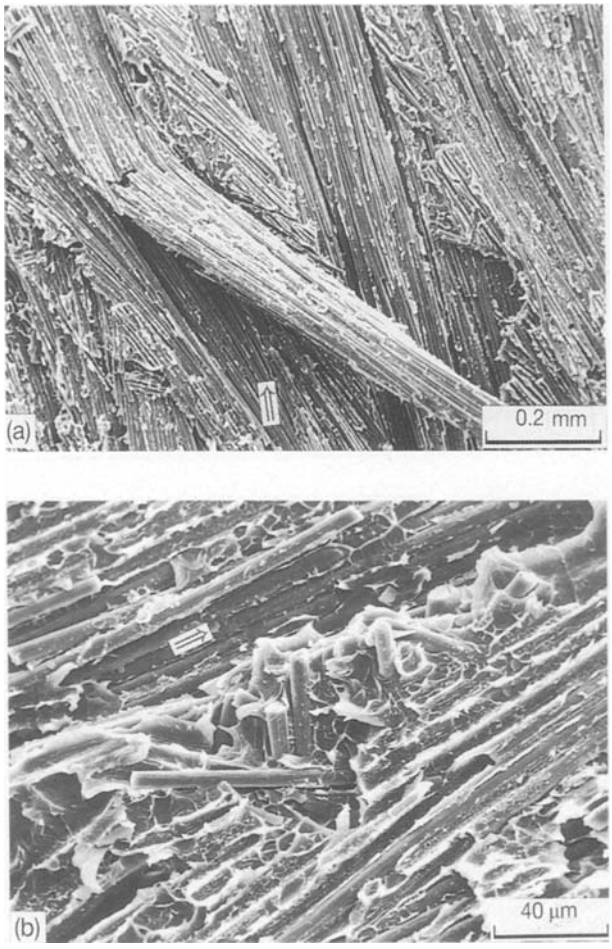


*Figure 13* SEM observation of the fracture surface of UD commingled composite. The arrow indicates the direction of crack propagation.

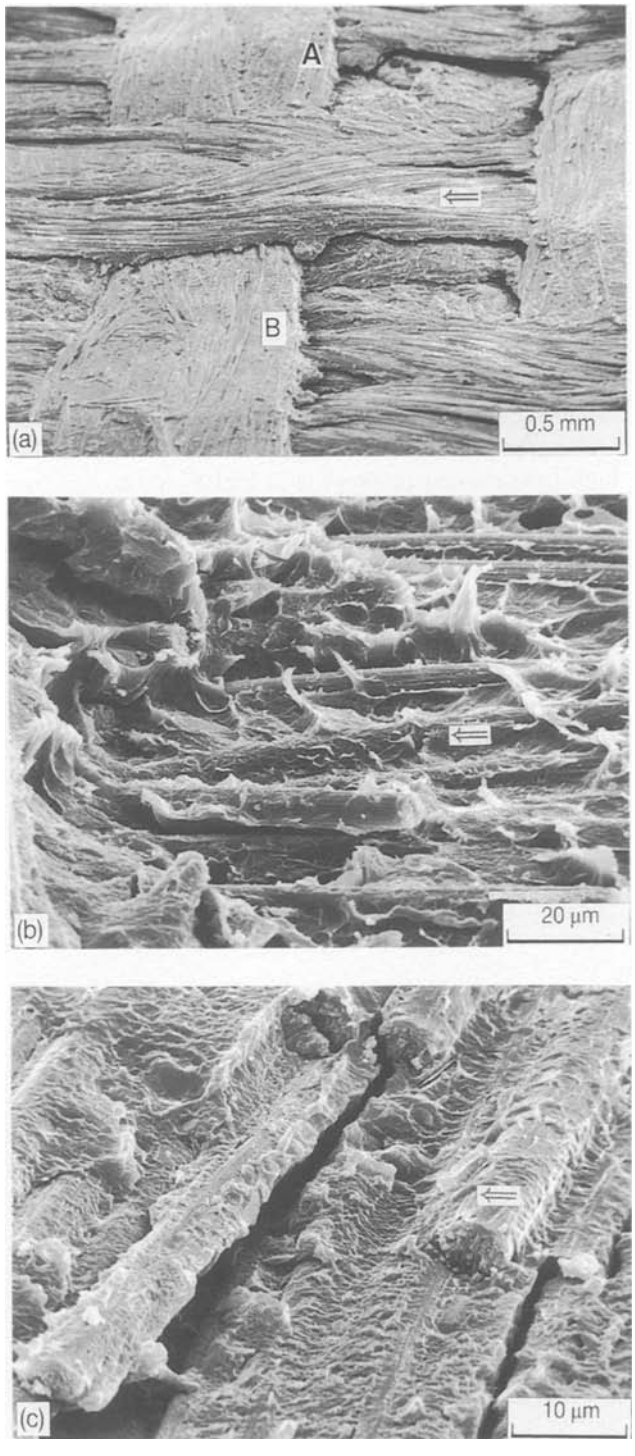


*Figure 14* SEM observation of the fracture surface of 2D commingled composite. (a) Whole view. (b) Ductilely fractured resin in front of the weft carbon fibres in the left edge. (c) Microductilely fractured resin on the surface of the weft carbon fibres.

times changes its plane of crack propagation as shown by A and B in Fig. 15a. This change of plane accompanies fibre breakage. Therefore, more energy may be dissipated than in the prepreg and the UD commingled composites where the delamination in a plane is dominant. The 2D commingled composite, therefore, exhibits a higher fracture toughness than the prepreg or the UD commingled composite. Fig. 15b is a magnification of the area around B in Fig. 15a.

We have attempted to measure the intralaminar fracture toughness [12]. Although it may not be reasonable to compare the absolute values because of the difference of the specimen's geometry, these results are summarized and compared with the interlaminar fracture toughness obtained here (Table III). The intralaminar fracture toughness of the unidirectional commingled composites is twice as high as the interlaminar fracture toughness. This may be due to the increase in the fibre bridging and/or fibre breakage in the intralaminar specimen [13].

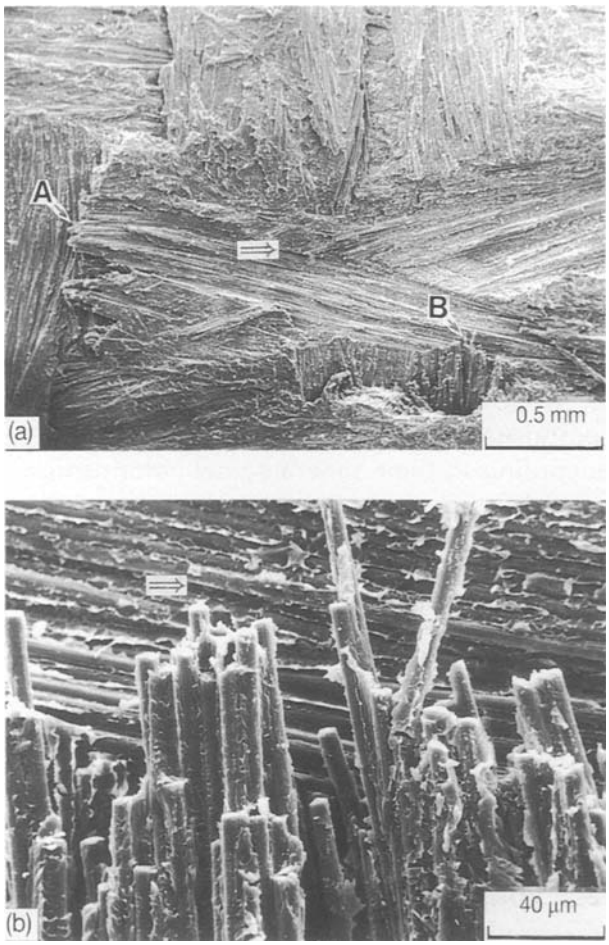


*Figure 15* SEM observation of the fracture surface of 2D commingled composite. (a) The change of delamination plane. (b) Magnification of the area around B in (a).

TABLE III Comparison of interlaminar fracture toughness with the intralaminar fracture toughness. The intralaminar data have been measured by the authors but these are not yet published

| Composite | Critical strain energy release rate ($J\,m^{-2}$) | |
|---|---|---|
| | Interlaminar | Intralaminar |
| CF/PEEK prepreg | 1560 | 3330 |
| UD commingled | 1980 | 4500 |
| 2D commingled | 2670 | – |
| CF/epoxy prepreg | – | 720 |

## 4. Conclusions

The unidirectional commingled composites have been shown to exhibit a higher fracture toughness than the prepreg composite. This is due to the poor fibre alignment. The misalignment of fibres interrupts the straight propagation of the crack, and there is a much greater chance for the fibres to bridge. In the case of 2D commingled composite where carbon fibres are both in the warp and the weft, the propagating crack is arrested before it passes through the weft carbon fibres and the crack propagation becomes unstable. Furthermore, the crack tends to propagate through the neighbouring laminae, thereby forming another crack propagation plane. Therefore, the fracture toughness of the 2D commingled composite was the highest. The impregnation of PEEK resin into the carbon fibres and the adhesion between them were excellent for all three types of composite. As a conclusion, the commingled yarn has the potential to improve the fracture toughness of the CF/PEEK composite.

## Acknowledgement

The authors appreciate the test materials donated by Mr Kunio Tanakamaru, the Director, Central Research Laboratory, Shikibo Ltd.

## References

1. I. Y. CHANG, *SAMPE Q.* **19** (1988) 29.
2. J. T. HARTNESS, *SAMPE J.* September/October (1984) 26.
3. A. C. HANDERMANN, in "20th International SAMPE Technical Conference", Minneapolis, 27–29 September (1988) p. 681.
4. A. Y. LOU, T. P. MURTHA, J. E. O'CONNOR and D. G. BRADY, in "Thermoplastic Composite Materials", edited by L. A. Carlsson (Elsevier Science, New York, 1991) p. 183.
5. K. HUKUDA, *Kyoka Plastics* **32** (1986) 160 (in Japanese).
6. S. HASHEMI, A. J. KINLOCH and J. G. WILLIAMS, *J. Compos. Mater.* **24** (1990) 918.
7. L. B. ILCEWICZ, P. E. KEARY and J. TROSTLE, *Polym. Engng. Sci.* **28** (1988) 592.
8. K. KAGEYAMA, T. KOBAYASHI and T.-W. CHOU, *Composites* **18** (1987) 393.
9. J. W. GILLESPIE Jr, L. A. CARLSSON and A. J. SMILEY, *Compos. Sci. Tech.* **28** (1987) 1.
10. J. P. BERRY, *J. Appl. Phys.* **34** (1963) 62.
11. S. L. BAZHENOV, *Composites* **22** (1991) 275.
12. H.YOON and K. TAKAHASHI, in preparation.
13. P. J. HINE, B. BREW, R. A. DUCKETT and I. M. WARD, *Compos. Sci. Tech.* **33** (1988) 35.

*Received 13 December 1991*
*and accepted 11 August 1992*